Anisotropy of thermal diffusivity of uniaxial stretched polyethylenes

H. G. Kilian and M. Pietralla

Universität Ulm, Abteilung Experimentelle Physik I, Oberer Eselsberg, D 7900 Ulm, West Germany

(Received 6 December 1976; revised 26 January 1978)

We have measured the dependence of the anisotropy ratio $A = \alpha_{\parallel}/\alpha_{\perp}$ of thermal diffusivity (at 300K) of polyethylene on the draw ratio, using a point source method. As crystallinity increases the anisotropy increases with the draw ratio. The measurements can be described with the aid of the well known aggregate model using the orientation parameters of the crystals as determined by X-ray methods which are not following an affine deformation assumption. Only one additional parameter is needed, the intrinsic anisotropy of a stack composed of alternating crystalline and amorphous lamellae. These stacks are regarded as the sub-units of deformation. The extrapolation of the intrinsic anisotropy yields reasonable results of $A \approx 2$ for the completely amorphous, and $A \approx 50$ for the completely crystalline polymers, respectively.

INTRODUCTION

Properties of oriented polymers as well as their deformation orientation processes have been studied extensively during the past few years. In spite of recognizing a remarkable amount of correlation in various interpretations, scarcely sufficient knowledge has been gained to answer all questions essentially concerned with the complicated cooperative processes that occur during deformation to larger extents.

It is hoped that some further progress in this direction may be made by an appropriate interpretation of the data obtained by the measurement of the anisotropy of thermal diffusivity at 300K of uniaxially stretched polyethylene having different degrees of crystallinity.

CLUSTER STRUCTURE

There is substantial evidence to indicate that organized superstructures exist within semicrystalline polymers. Small-angle X-ray patterns of melt crystallized polyethylene with varying degrees of crystallinity can quantitatively be interpreted in terms of idealized structural sub-units, the clusters, the sizes of which are in the range of several hundreds of angstroms[1–4]. An example of this kind of structure, given in a two-dimensional representation, is illustrated in *Figures 1* and *2*. The statistical nature of the structure is seen by SAXS characterization evidence which is in principle confined to the direction which is normal to the flat lamellae ('longitudinal direction')[4].

For the present purposes it is sufficient to note that the presence of the clusters gives evidence for local anisotropy on various physical properties. Some of these will be considered in the subsequent sections, with the aim of finding general concepts for treating the relationships between the given superstructure and its influence on macroscopic measurable quantities.

ORIENTED SAMPLES

Comparison of the cluster ensemble depicted in *Figure 2* with the structure of a molecular network reveals an interesting analogy. The unique structural feature common to both systems is the presence of long polymer chains which give rise to corresponding networks when crosslinking occurs[5]. We may imagine the deformation of a cluster network to be conducted in such a manner that affinity to the changes of the macroscopic shape may be imposed on the single clusters thus defining them as the 'sub-systems of deformation', the internal properties of which account for the macroscopic anisotropy in oriented systems due to the corresponding orientation and dilation of the sub-systems themselves.

From the quantitative description of the orientation distribution functions of higher deformed samples, the clusters are known to represent equally well sub-systems of deformation which are submitted to proper shear, as well as melting, and recrystallization processes[5–7].

Based on these results we use an aggregate model for the phenomenological description of the macroscopic properties of oriented semicrystalline systems. In this paper we are

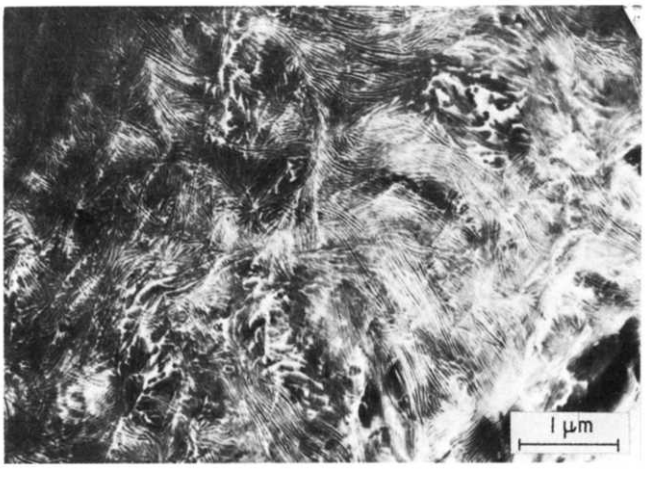

Figure 1 Electron micrograph of high density polyethylene[2]. There are always several lamellae running parallel forming 'clusters' where flat. The clusters are easily found by placing a proper grid upon the picture

0032–3861/78/1906–0664$03.00

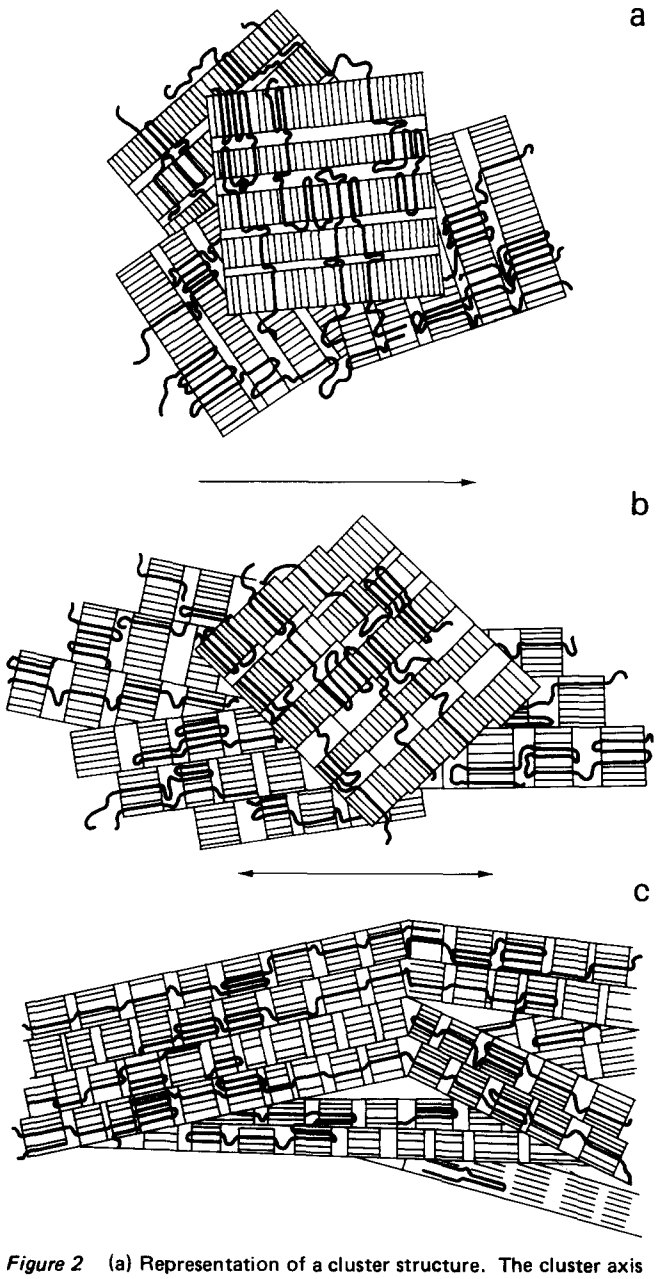

Figure 2 (a) Representation of a cluster structure. The cluster axis is defined by the crystal *c*-axis direction. The orientation within the amorphous layers is correlated to the *c*-axis of crystals. Behaviour of clusters during the stretching process: (b) At moderate draw ratios $1 < \lambda \lesssim 2 \sim 3$ ($\lambda = l/l_0$: l, actual; l_0, initial length of the sample) the clusters are mainly deformed by shear processes; (c) At high ratios $\lambda > 2 \sim 3$. The cluster size has been diminished by the local melting and recrystallization process. Further deformation takes place mainly between the clusters

substantially interested in the description of the anisotropy of thermal diffusivity (*ATD*) of various polyethylene samples with different degrees of crystallinity, looking for an appropriate characterization of dynamical internal properties of the stacks at temperatures well above the glass transition temperature of the amorphous phase.

ANISOTROPY OF THERMAL DIFFUSIVITY

The macroscopic diffusivity, α, of a homogeneous system is related to the conductivity, k, by:

$$\alpha = k/c_p\rho \tag{1}$$

where c_p is the heat capacity per unit mass and ρ is the density. On defining the macroscopic anisotropy, A, of systems with a symmetry axis, we arrive at the ratio:

$$A = \alpha_\parallel/\alpha_\perp = k_\parallel/k_\perp \tag{2}$$

where $\alpha_\parallel/\alpha_\perp$ is the macroscopic thermal diffusivity parallel and perpendicular to the axis of symmetry; recognizing that the anisotropy of the thermal diffusivity identifies with the analogue ratio of heat conductivities.

AGGREGATE MODEL

The macroscopic sample is considered now to be composed of an ensemble of stacks, the average principle diffusivities of which should be defined by $\alpha_{i\parallel}$ and $\alpha_{i\perp}$, respectively. The suffix i is added as a reminder that the above symbols are related to the stacks as intrinsic properties. On describing the macroscopic anisotropy of an ensemble of stacks with uniaxial orientation, we use the series model, i.e. the additivity of the resistivities; of the two linear approaches (parallel and series models respectively) this has been found to be the more accurate one. Moreover, as the error involved in the series model is a systematic one, the error of the calculated anisotropy *ratio* becomes much smaller. If the percentage errors in calculating $\alpha_\parallel$ and $\alpha_\perp$ were equal, which is very likely for various physical reasons, the ratio derived would be exact! Therefore, there is no need for a more refined treatment as this would be a case of calculating the absolute values.

This method would provide the direct route and recently Choy and Young[23] have made a new attack on this problem with reasonable success. But this approach has its limitations – as all composite models hitherto – from the lack of knowledge of single phase properties, interrelations and structure dependence. In contrast, our method is to look for structure units with invariant behaviour with respect to the properties under discussion, and then try to analyse the orientation behaviour of these units during deformation.

With the resistivity tensor components:

$$\alpha^{ij} = (-1)^{i+j}\,\Delta^{\alpha}_{ij}/\det(\alpha_{ij}) \tag{3}$$

where $\Delta^{\alpha}_{ij} = \alpha_{ij}$, minor of (α_{ij}) and α_{ij} is the diffusivity tensor. Equation (3) reduces to $\alpha^{ii} = 1/\alpha_{ii}$ for orthorhombic symmetry. We arrive at the following expressions for the resistivities perpendicular, $\alpha^\perp$, and parallel, $\alpha^\parallel$, to the draw direction at angles ϕ and θ inclined to the symmetry axis of the stack:

$$\alpha_1^\perp = \alpha^{11} = (\alpha_i^\parallel - \alpha_i^\perp)\sin^2\theta\cos^2\phi + \alpha_i^\perp \tag{4}$$

$$\alpha_2^\perp = \alpha^{22} = (\alpha_i^\parallel - \alpha_i^\perp)\sin^2\theta\sin^2\phi + \alpha_i^\perp \tag{5}$$

$$\alpha^\parallel = \alpha^{33} = \alpha_i^\parallel\cos^2\theta + \alpha_i^\perp\sin^2\theta \tag{6}$$

with $\alpha_i^\parallel = \alpha_i^{33}$ and $\alpha_i^\perp = \alpha_i^{22} = \alpha_i^{11}$. Referring to the rotational symmetry of the orientation pattern with respect to the draw direction, the functions $\cos^2\phi$ and $\sin^2\phi$ may be replaced by their average values $\langle\cos^2\phi\rangle = \langle\sin^2\phi\rangle = 1/2$. Integration over all directions, θ, which denotes the angle between the symmetry axis of the stacks and the draw direction, then yields:

$$\alpha^\perp = \tfrac{1}{2}[(\alpha_i^\parallel + \alpha_i^\perp) - (\alpha_i^\parallel - \alpha_i^\perp)\langle\cos^2\theta\rangle] \tag{7}$$

$$\alpha^\parallel = (\alpha_i^\parallel - \alpha_i^\perp)\langle\cos^2\theta\rangle + \alpha_i^\perp \tag{8}$$

with

$$\langle\cos^2\theta\rangle = \int_0^{\pi} F(\theta)\cos^2\theta\sin\theta\,d\theta \Big/ \int_0^{\pi} f(\theta)\sin\theta\,d\theta \qquad (9)$$

where $F(\theta)$ is the orientation density distribution of the symmetry axis of the stacks with respect to the draw direction.

With these equations, the macroscopic measurable anisotropy of thermal diffusivity, A, can be expressed as:

$$A = \frac{\alpha^{\perp}}{\alpha^{\parallel}} = \frac{1}{2}\left\{\frac{2A_i + 1}{A_i - (A_i - 1)\langle\cos^2\theta\rangle} - 1\right\} \qquad (10)$$

where A_i is consequently given by $A_i = \alpha_i^{\perp}/\alpha_i^{\parallel} = \alpha_{i\parallel}/\alpha_{i\perp}$. In principle, allowing for a dependence on the draw ratio according to:

$$\alpha_i^{\parallel}(\lambda) = q(\lambda)\alpha_{i0}^{\parallel} \qquad \alpha_i^{\perp}(\lambda) = q(\lambda)\alpha_{i0}^{\perp} \qquad (11)$$

where $\alpha_{i0}^{\parallel}$ and $\alpha_{i0}^{\perp}$ refer to the unstretched sample, A_i is found to be invariant, thus yielding a dependence of A on the second moment of the orientation distribution function only. *In discussing* A_i, *it is to be noted that this quantity should, in principle, be dependent on the internal dynamic properties of the stacks, to the origin of which our interests are mainly directed, stressing essentially the point of whether there is any dynamic cooperation between the structural elements of the stack.*

METHOD OF DE SERNAMONT

De Sérnamont[8] first demonstrated *ATD* with the isotherms due to a heat point source. We will consider the mathematics of his treatment.

From the partial differential equation with constant coefficients formulated in Cartesian coordinates:

$$\frac{\partial T}{\partial t} = -\sum_{ij}^{N} \alpha_{ij}\frac{\partial^2 T}{\partial x_i\,\partial x_j} + \hat{Q}_N(\vec{x}') \qquad (12)$$

where T is the temperature; α_{ij} are elements of the diffusivity tensor; x_i is the coordinate in direction of the principal axis i; t is time; N is the number of spatial dimensions; Q is the rate of heat production; $\hat{Q}_N = Q/\rho_N c_p$ and ρ_N is a 3- or 2-dimensional mass–density. We are led to the particular solution for $x_i \neq x_i'$ and $t \neq t'$ (Greens function)[9,10]:

$$G(\vec{x}, t|\vec{x}', t') = [\det(\alpha^{ij})]^{1/2}[4\pi(t-t')]^{-N/2}\exp\{-R^2/4(t-t')\} \qquad (13)$$

with

$$R^2 = \sum_{1}^{N} \alpha^{ij}(x_i - x_i')(x_j - x_j') \qquad N \geqslant 2 \qquad (14)$$

where an instantaneous heat point source of unit power is assumed to be located at $(\vec{x}', t')$. If the initial temperature of the infinitely extended systems equals the value of $T = 0$, the temperature pattern which refers to a definite period of heating with the aid of a source covering a definite, but small part of the sample is given by:

$$T(\vec{x}_1 t) = \int_0^{t} dt' \int_{\Omega_N} Q_N(\vec{x}', t')G(\vec{x}, t/\vec{x}', t')\,d\Omega_N(\vec{x}') \qquad (15)$$

which does not take surface terms into consideration; allowance for these is made by the assumption of a sufficiently large volume, Ω_N, as well as a sufficiently short period of heating. The influence of macroscopic boundary conditions due to the limited dimensions of the sample is indicated in the Appendix I. In order to render equation (15) in a usable form, in which allowance is made for the calculation of the isotherms $T(\vec{x})$ = constant, it is necessary to consider an infinitely small heat source located at the origin with constant heat production, according to $\hat{Q}(\vec{x}', t') = \hat{Q}\delta(\vec{x}')$ where $\delta(\vec{x}')$ where $\delta(x')$ denotes Dirac's delta function. Integration over the period of time with $t' = 0$ finally yields:

$$T = \frac{\hat{Q}_3}{4\pi}\det(\alpha^{ij})^{1/2}R^{-1}\mathrm{erfc}\{R/(4t)^{1/2}\} \qquad (16)$$

for $N = 3$

$\mathrm{erfc}(x) = 1 \quad \mathrm{erf}(x)$; $\mathrm{erf}(x)$ = error function

and

$$T = -\frac{\hat{Q}_2}{4\pi}\det(\alpha^{ij})^{1/2}E_i(-R^2/t) \qquad N = 2 \qquad (17)$$

with $E_i(x)$ denoting the integral–exponential function. Taking the principal axes as the system of coordinates we learn from equations (16) and (17) that the isotherms $T(\vec{x})$ = constant are represented in both cases by the same family of ellipsoids:

$$\sum_{i}^{N} \alpha^{ij}x_i x_j = \sum_{1}^{N}\frac{x_i^2}{\alpha_{ii}} = \text{constant} \qquad (18)$$

Denoting the principal axes of the ellipsoids by r_i we are led immediately to the equation:

$$A = \alpha_{ii}/\alpha_{jj} = (r_i/r_j)^2 \qquad N = 2.3 \qquad (19)$$

Hence, it is only necessary to record the isotherms 'visible' in order to calculate A according to equation (19).

MEASUREMENTS

The experimental set up is shown in *Figure 3a*. As heat source a heated metal cylinder of small diameter is in contact with its flat front area at a position in the centre of the surface of the slab for a certain period of time. Cholesteric liquid crystals are used as indicators for the optical display of isotherms within an accuracy of ±0.1K (for more details see Appendix II). A representative example of a photographed pattern is shown in *Figure 3b*.

The available data for the polyethylene involved are listed

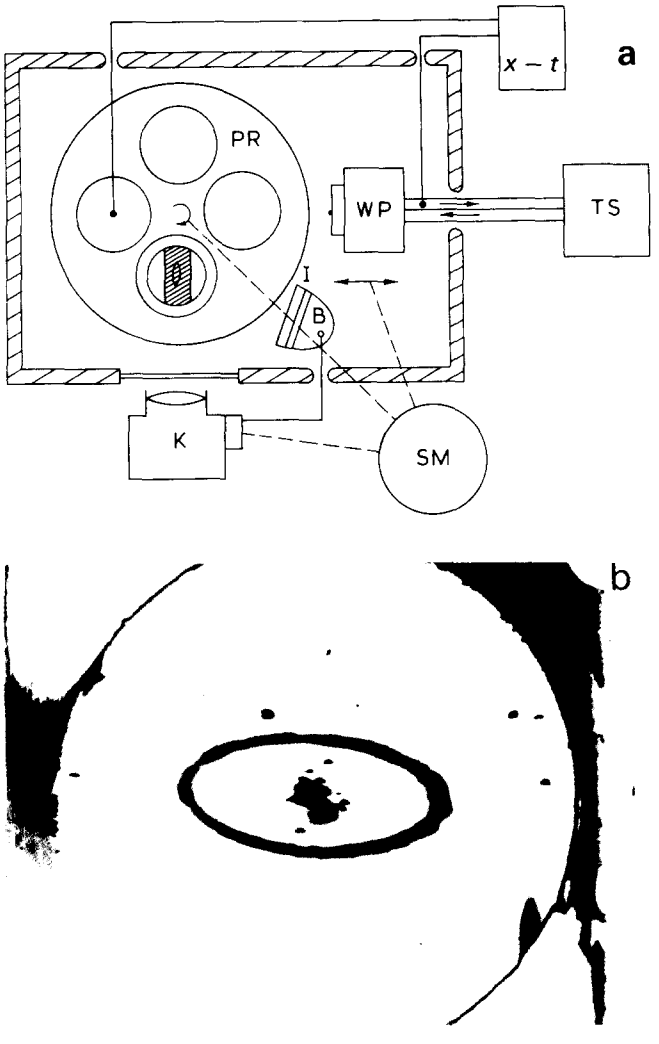

Figure 3 (a) Experimental set-up. The sample is in contact with the heat point source, WP, the temperature of which is controlled by a thermostat, TS. It is brought in front of the photographic camera, K, by means of a sample revolver, PR, containing 4 samples. The picture is taken with flash light illumination, B, through an interference filter, I, in order to select a proper isotherm. The temperature of the samples and the heat point source is recorded by an *X-t*-recorder. All mechanical operations are carried out by a motor driven device, SM. (b) Example of an isotherm recording; photographic negative (low density PE: $\lambda = 4.8$, $A = 5.3$)

in *Table 1*, illustrating the systematic variation of the degree of crystallinity.

RESULTS

From the results illustrated in *Figures 4a–4d* a systematic dependence of A, measured at 318K, on the draw ratio, λ, as well as on the degree of crystallinity is confirmed. The slope of $A(\lambda)$ increases considerably with increasing values for the degree of crystallinity, w^c, thus yielding the maximum anisotropy of thermal diffusivity for high density polyethylene.

$k_\parallel$ and $k_\perp$ have been measured by Hansen and Bernier[11] using an absolute method. Considerable agreement with the data obtained in this paper is demonstrated by comparison with *Figure 4a*. Results published by Novichyonok[12] are not as much in conformity with these data, thus a quantitative comparison cannot be made as successfully due to the lack of the necessary data.

PHENOMENOLOGICAL REPRESENTATION

It appeared to be profitable to represent the measured $A(\lambda)$ in terms of the $\langle\cos^2\theta\rangle$ values which have been computed for the c-axis in the crystals from the appropriate X-ray measurements[13]. It is demonstrated in *Figure 5* that a surprisingly accurate fit of the experimental data can be obtained with the aid of equation (10), assigning A_i to constant values which must only be considered to be a function of the degree of crystallinity. The values of $A_i(w^c)$ assigned to the various polyethylene samples by the fit of the experimental data, are listed in *Table 1*. The smoothed function $f_{cv}(\langle\cos^2\theta\rangle)$ employed in the above calculations, is plotted in *Figure 7*.

DISCUSSION

The tendency to attribute the regularities of the deformation behaviour of semicrystalline polymers to common properties of the superstructure receives substantial support from the observed independence of $A_i(w^c)$ on the draw ratio. Its invariance is equally well maintained for samples that after being unloaded, have been relaxed into a state with a correspondingly reduced value of the draw ratio as indicated in *Figure 4d*.

In view of the exceedingly large A_i which might appear according to the data shown in *Table 1*, an 'affine' dependence as formulated in equation (11) would be difficult to examine with the aid of the aggregate model. Thus, we arrive at the statement that $\alpha_{i\parallel}$ and $\alpha_{i\perp}$ should be considered to be fairly independent of the draw ratio*.

It appears almost axiomatic that the value assigned to A_i in a semicrystalline polymer system should primarily be dependent on the locally established orientational correlations. Clearly, these correlations might then be characterized by the average number N_L of crystal lamellae within the original clusters by means of the simple relation[15]:

$$N_L = 1 + b[w^c/(1 - w^c)] \tag{20}$$

where b has been assigned the value 1.7. The above equation is obtained only if the average width of the lamellar shaped crystals, $\langle y_b\rangle$, is definitely related to the average thickness, $\langle y_c\rangle$ according to $\langle y_b\rangle = b\langle y_c\rangle$. From the above we are led to define the following formulation:

$$A_i(w^c) = N_L A_{i0} \tag{21}$$

where A_{i0} represents the limiting value of $A_i(w^c)$ for $N_L = 1$, corresponding to a system with the asymptotic value of $w^c = 0$. We learn from *Table 1* that the characteristic dependence of A_i on w^c can easily be computed if A_{i0} has been adjusted by fitting the experimental A_i obtained for low density PE.

Thus we have obtained the striking result that the orientational correlations which have been locally established during the crystallization should depend on the degree of

* This is in accordance with the statement of Choy and Greig[14] that the boundary resistance of the crystalline–amorphous interfaces which are induced during the deformation should be very small at these high temperatures.

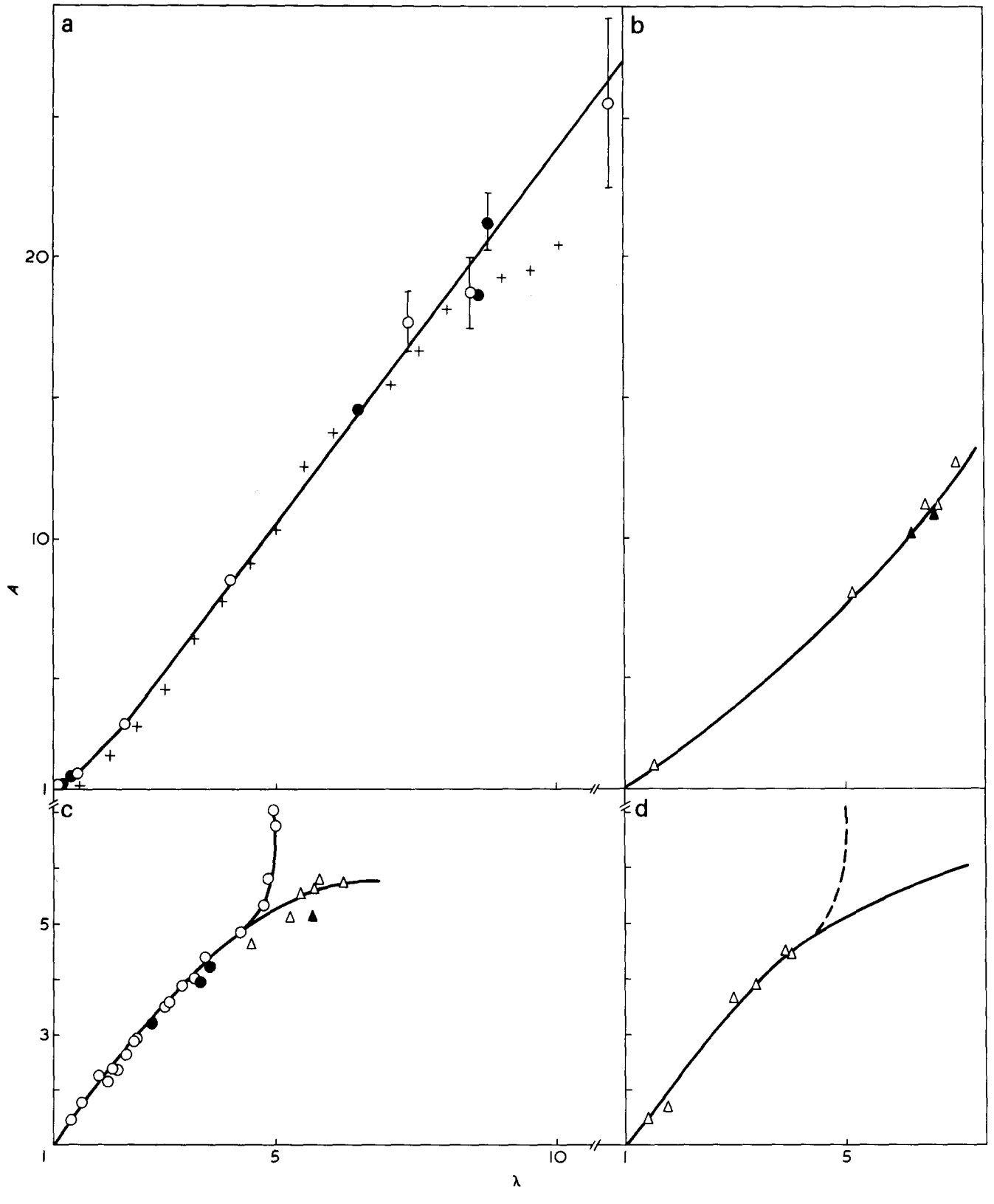

Figure 4 Measurements of anisotropy of thermal diffusivity. T_s, stretching temperature: $\dot{\epsilon} = l_0^{-1} \times dl/dt$, stretching rate, w_c, crystallinity. (a) High density PE: $w_c = 0.82$; $T_s = 85°C$; $\dot{\epsilon} = 5 \times 10^{-6} sec^{-1}$. ○, samples under stress; ●, relaxed samples; +, calculated from measurements of Hansen and Bernier[11]. (b) Ziegler–Natta type PE: $w_c = 0.69$; $T_s = 65°C$; $\dot{\epsilon} = 5 \times 10^{-6} sec^{-1}$. △, Samples under stress; ▲, relaxed samples. (c) Low density PE: $w_c = 0.42$. ○, $T_s = 31°C$, $\dot{\epsilon} = 5 \times 10^{-6}$–$1 \times 10^{-5} sec^{-1}$, samples under stress; ●, $T_s = 31°C$, $\dot{\epsilon} = 8 \times 10^{-4} sec^{-1}$, relaxed samples; △, $T_s = 85°C$, $\dot{\epsilon} = 10^{-5} sec^{-1}$, samples under stress; ▲, $T_s = 85°C$, $\dot{\epsilon} = 10^{-5} sec^{-1}$, relaxed samples. The increase at $\lambda \sim 5$ ($T_s = 31°C$) is attributed to stress-induced crystallization. (d) Low density PE: $w_c = 0.42$. (———), Best fit curve from *Figure 4c*. These are measurements at samples stretched at $T_s = 22°C$, with $\dot{\epsilon} = 8 \times 10^{-4} sec^{-1}$, which have been relaxed for two days at room temperature

crystallinity only and remain unaltered during the deformation, in spite of well established systematic changes of the superstructure (as indicated in the first sections of the paper).

Equation (21) allows for an estimate of the limiting values

Table 1

Samples	L 1810 D®	L 5041 D®	L 6041 D®
Density (g/cm^3)	0.918	0.950	0.960
Melt index (g/10 min) (MFL 190/2.16)	0.2	0.2	0.2
w^c [a]	0.43	0.69	0.82
$N_L(w^c)$	2.2	4.8	8.7
$A_i(w^c)$(experimental)	7	16	26
$A_i(w^c)$(theoretical)	7[b]	15	27.5

[a] Determined by X-ray method[16]; [b] fitted using equation (21), giving $A_{i0} = 3.15$

of $A_i(w^c)$ giving $A_{i0} = 3.15$ as the elementary anisotropy of the thermal diffusivity for a non-crystallized system without any orientation correlation which is in good correspondence with values assigned to the chain segments of non-crystallized polymers[17]. The extrapolation in *Figure 6*, $w_c \to 0$, yields the lower value of 1.7–1.9 which is in accordance with measurements of oriented vinylic polymers in the glassy state[18,19]. On the other hand, A_{i0} takes infinitely large values in the limit of $w^c \to 1$ indicating that a refinement of the considerations is needed as far as energy density is concerned.

An advanced discussion of the phonon spectrum in the systems under discussion is required. Despite this shortcoming it is evident that exceedingly high values for the anisotropy of thermal diffusivity of a polymer single crystal must be expected which must have at least the same order of magnitude as those obtained for pyrolithic graphite (A_i = 200–250)[20].

STRESS-INDUCED CRYSTALLIZATION

Since the anisotropy of the heat conduction of the stacks, A_i, depends on the degree of crystallinity, any stress-induced crystallization should clearly be indicated by a corresponding change of the slope of $A(\lambda)$. Indeed $A(\lambda)$ of low density polyethylene observed under stress at ambient temperature, departs from the expected curve at a sufficiently large draw ratio on these grounds (see *Figure 4c*).

The sudden increase of $A(\lambda)$ should be governed by a continuous stress-induced crystallization because of the stabilization of the smallest extended-sequence crystals. Using the approximate equation[21]:

$$w^c = x_c^{y_{\min}}(1 - H/3) \qquad H = 0.15 \qquad (22)$$

where $y_{\min}$ is the minimum average thickness of the sequence extended mixing crystals and $x_c = 0.95$ = the mole fraction of the 'crystallizable co-units' (CH_2 groups in the case of the

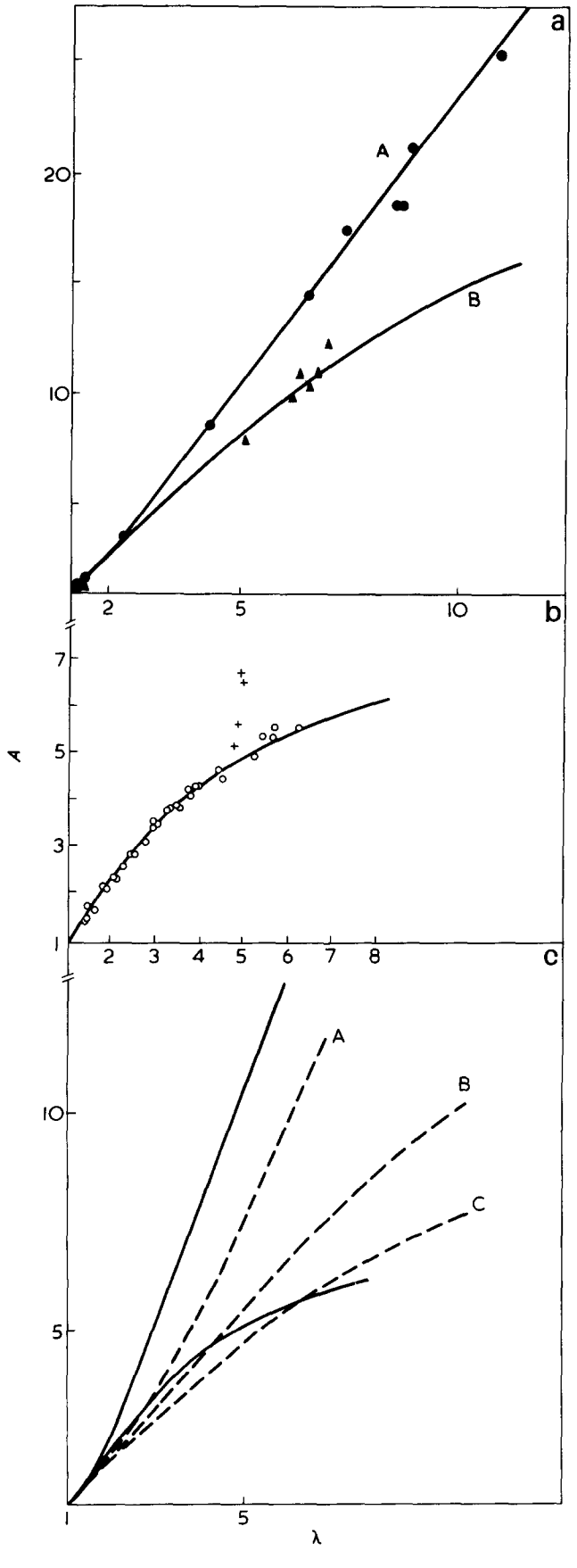

Figure 5 Anisotropy of thermal diffusivity calculated using equation (10) and the orientation parameter of the crystals (smoothed curve of *Figure 7*). The A_1 are the intrinsic anisotropies of the clusters. (a) A, HDPE A_i = 26; B, MDPE (Ziegler–Natta type) A_i = 16, (b) LDPE, the crosses indicate the occurrence of stress crystallization. A_i = 7. (c) (– – – –), Calculated from equation (10), with the orientation parameters of the affine deformation model. The intrinsic anisotropies used are indicated. A, ∞; B, 20; C, 12. From the measurements on LDPE and HDPE respectively, it is clearly seen that the affine orientation assumption completely fails in the description of the experiments. Comparing the curve for HDPE with the calculation for $A_i \to \infty$, the influence of orientation on the macroscopic anisotropy is demonstrated

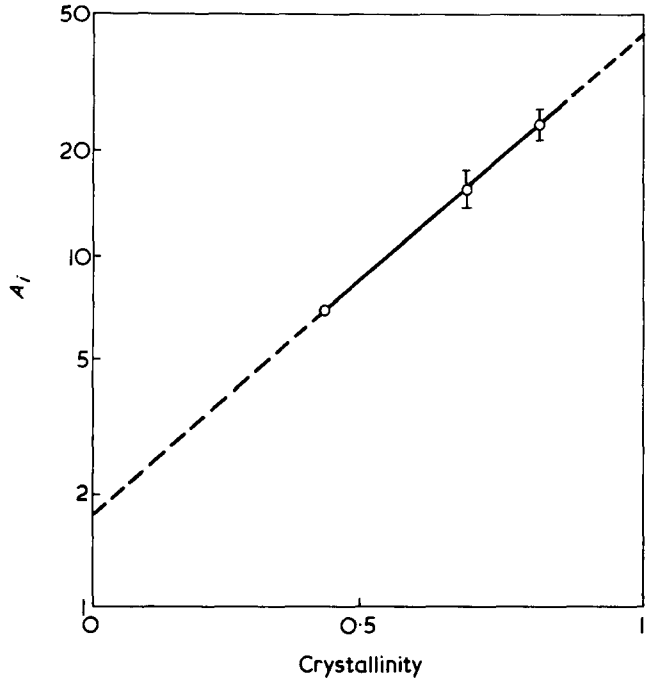

Figure 6 Plot of the intrinsic anisotropy of the clusters *versus* crystallinity

Table 2

A_i	w^c_{theor}	Δw^c	γ_{min}
7.6	0.45	0.03	15
8.4	0.50	0.08	13
10.4	0.58	0.16	10
11.1	0.60	0.18	9

low density polyethylene) where the non-crystallizing units are represented by short-chain branches, we may estimate the change in degree of crystallinity and find the reasonable values assigned to γ_{min} which are listed in *Table 2* with a maximum change in w^c of about 0.20.

The values w^c_{theor} are computed by fitting the observed $A(\lambda)$ using equation (10) and $\langle\cos^2\theta\rangle$ derived from the smoothed curve assuming that further crystallization takes place within the stacks.

The accuracy of this interpretation is supported by the observations that the stress-induced crystals melt on thermodynamic grounds if the sample is unloaded, or they do not appear at all if the deformation is carried out at higher temperatures. In the latter case no anomaly in the slope of $A(\lambda)$ is obtained as shown in *Figure 4c*.

CONCLUSIONS

Although a quantitative assessment of all the details cannot be given, a fundamental understanding of the above phenomena can be put forward employing the cluster network model. For these purposes it seems profitable to recall the fact that the *chain vectors* of an ideal molecular network on which an affine deformation is imposed will uniquely be deformed according to the 'master function'.

$$f(\theta) = \lambda^3[1 + (\lambda^3 - 1)\sin^2\theta]^{-3/2} \qquad (23)$$

This is equally valid for each molecular network, independent of its special structure, and thus yields the same $\langle\cos^2\theta\rangle$ function for the chain vectors themselves.

To avoid possible misunderstanding it should be said that the orientation of the segments of a molecular network with an affine deformation of the junction points is not an affine one but depends on the structure of the chains† (e.g. number of segments). In this case the chains represent the subsystems of deformation with internal possibilities of orientation and it is this internal behaviour of the sub-system chosen which has to be described by a proper model.

The affine orientation function is not valid for crystalline polymers, i.e. we cannot identify the 'chain vectors' with the crystal *c*-axes. Moreover, the orientation distribution function of the crystal *c*-axes differs severely from the affine one[5,13]. This behaviour also appears in our measurements if we try to calculate the anisotropy by use of the affine orientation parameters (see *Figure 5c*).

On the other hand it is clearly seen from *Figure 7* that for f_{cv}, computed from the $A(\lambda)$ identical measurements are obtained for all systems of *any degree of crystallinity whatever.*

The orientation parameters of the crystals determined by X-ray wide-angle scattering compare quite favourably with this curve even in the case of a slightly crystallized ($w_c \leqslant 0.1$) poly(vinyl chloride)[18]. This master curve clearly reflects the orientation processes of a two phase polymer to which the system is forced by the existence of crystallites, in contrast to the orientation behaviour of the segments of amorphous polymers (shaded area in *Figure 7*).

From the existence of the master curve, the idea of taking the clusters as the sub-systems of deformation of a cluster network is readily confirmed, where we assume a modified affine transformation law for the 'chain vectors'.

Nevertheless the internal orientation and dilation within the corresponding sub-systems (e.g. *c*-axes of the crystals) will be substantiated by shearing, sliding, partial melting and

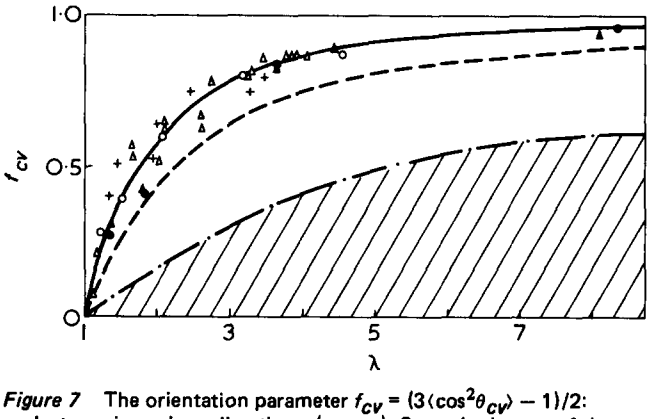

Figure 7 The orientation parameter $f_{cv} = (3\langle\cos^2\theta_{cv}\rangle - 1)/2$: *c*, cluster axis, *v*, draw direction. (———), Smoothed curve of the crystal parameters as used in the calculation of *Figure 5*. (— — —), Represents the affine deformation scheme. The symbols are measured values of crystal *c*-axis

Sample		Reference
● LDPE ▲ HDPE	Under stress	13
△ HDPE ○ LDPE	Relaxed	5
+ PVC	Relaxed	18

† Only the 'chain vectors' obey the affine orientation function (equation 23).

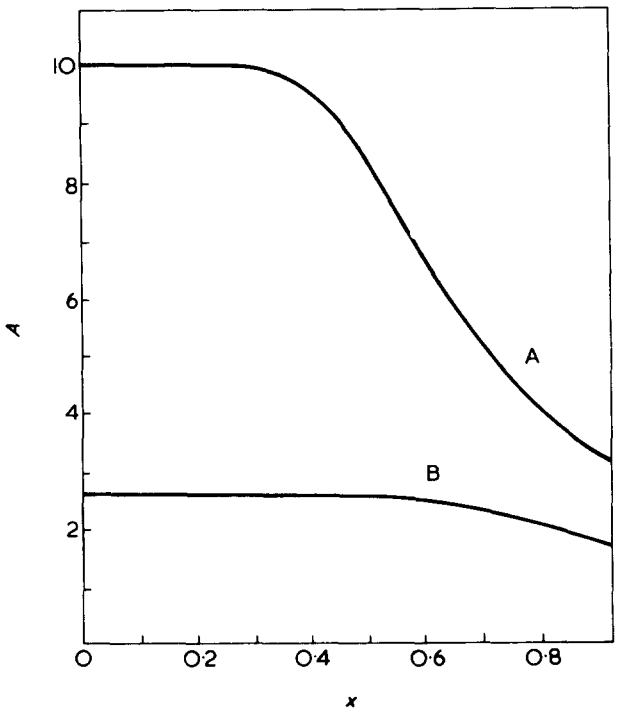

Figure 8 Influence of boundary conditions. The ends of the samples (in the stretching direction) are kept at constant temperature, the sides of the samples are thermally isolated. Thus the anisotropy determined by equation (19) depends on the relative diameter $x = r_\perp/b$ of the isotherms perpendicular to the draw direction (small axis of the ellipse). b denotes the width of the samples; A_0 is the exact anisotropy of the material. The length to width ratio was $l/b = 2$. A, $A_0 = 10$; B, $A_0 = 2.5$

recrystallization and may greatly deviate from an affine deformation assumption.

Thus, further analysis of the factors governing the deformation processes wtihin the clusters in semicrystalline polymer systems should at least lead to a unique and generally valid classification whereby the interrelations between the dynamic properties and the superstructure afford some deeper considerations. But this is out of the scope of this work and will be discussed in further communications.

ACKNOWLEDGEMENT

The authors thank BASF for providing the polymers, and the Deutsche Forschungs-Gemeinschaft for financial support.

REFERENCES

1 Geil, P. H. 'Polymer single crystals' Wiley–Interscience, New York, 1963; Wunderlich, G. 'Macromolecular Physics' Academic Press, London–New York, 1973
2 Kanig, G. *Prog. Colloid Polym. Sci.* 1975, **57**, 176
3 Wenig, W. and Kilian, H. G. *Macromol. Phys. (B)* 1974, **9**, 463
4 Meyer, H. and Kilian, H. G. *Prog. Colloid Polym. Sci.* in press
5 Kilian, H. G., Heise, B. and Pietralla, M. *Prog. Colloid Polym. Sci.* 1977, **62**, 16
6 Fischer, E. W. *Kolloid Z. Z. Polym.* 1968, **231**, 458
7 Martis, K. -W. and Wilke, W. *Colloid Polym. Sci.* 1977, **62**, 44
8 De Sénarmont, H. *Pogg. Ann.* 1848, **73**, 191; 1849, **74**, 190; 1849, **75**, 50
9 Carslaw, H. S. and Jaeger, J. C. 'Conduction of Heat in Solids', Clarendon Press, Oxford, 2nd Edn, 1959
10 Chang, Y. P., Kang, C. S. and Chen, D. J. *Int. J. Heat Mass Transfer* 1973, **16**, 1905
11 Hansen, D. and Bernier, G. A. *Polym. Eng. Sci.* 1972, **12**, 204
12 Novichyonok, L. N. *Prog. Heat Mass Transfer* 1973, **5**, 293
13 Heise, B. *Thesis*, University of Ulm (1972)
14 Choy, C. L. and Greig, D. *J. Phys. (C)* 1975, **8**, 3121
15 Kilian, H. G. and Klattenhoff, D. *Colloid Polym. Sci.* in press
16 Hendus, H. and Schnell, G. *Kunststoffe* 1961, **5**, 69
17 Eiermann, K. *Kolloid Z. Z. Polym.* 1964, **201**, 3
18 Hellmuth, W., Kilian, H. G. and Müller, F. H. *Kolloid Z. Z. Polym.* 1967, **218**, 10
19 Hellwege, K. H., Hennig, J. and Knappe, W. *Kolloid Z. Z. Polym.* 1962, **188**, 2; Washo, B. D. and Hansen, D. *J. Appl. Phys.* 1969, **40**, 6
20 Hooker, C. N., Ubbelohde, A. R. and Young, D. A. *Proc. Roy. Soc. (A)* 1965, **284**, 17; Taylor, R. *Phil. Mag.* 1966, **13**, 157
21 Kilian, H. G. and Stracke, F. *Colloid Polym. Sci.* in press
22 Fergason, J. L. *Appl. Opt.* 1968, **7**, 1729
23 Choy, C. L. and Young, K. *Polymer* 1977, **18**, 769

APPENDIX I

As our samples are clamped into the sample holder under stress or in the relaxed state, the sides of the samples are free of contact with other material, whereas the ends are always in tight contact with the metal clamps. As a consequence the boundary conditions are to a good approximation $T = T_0$ (constant) at the ends, and zero heat flux across the sides of the plate-like samples. These conditions are achieved mathematically by placing two image sources at a distance $\pm b/2$ from the sides, and two image sinks at a distance of $\pm l/2$ from the ends, where b and l denote the width and the length of the sample respectively. All sinks and sources as given by (17) are equal in strength. As a result the form of the isotherms is mainly affected by their distances from the sides of the sample and not by the heating rate or heating time. For isotherm diameters less than 1/3 of the corresponding sample dimension we may further use (17) and (19) respectively for calculations, the error introduced being less than the uncertainty in measuring the isotherm diameters.

A representative example for the influence of the boundary conditions is shown in *Figure 8* where parameters from our experiments have been used.

APPENDIX II

By shaping the heat source as a truncated cone, a maximum heat flux into the sample is established for a definite temperature gradient, ΔT.

Using a thermostat with sufficient circulation due to a bypass in the mounting of the cone, the temperature in the cone was controlled to within ±0.1°C.

Recording of the isotherms

Cholesteric liquid crystals are used as indicators offering an attractive method for the optical display of isotherms with an accuracy of 0.1°C, 2×10^{-3} cm and 0.1 sec[22].

The surface of the sample should be black. Since a cholesteric liquid does not absorb light, but scatters it selectively, it is necessary to absorb that light which is not scattered. This condition is met by applying a black dye. Finally, the liquid crystal is coated on the sample using a brush and then heated beyond T_2 for formation. In the centre of the sample an area of 2 mm in diameter is liberated from the coating in order to obtain a direct contact between the cone and the sample. The liquid crystal must always be freshly coated because after 3–4 h the film surface may become marred, if it is exposed to the air.

A xenon flash light was chosen for illumination. To select

an isotherm, a narrow band-pass filter for the blue xenon line at 467.1 nm was used Additionally, the filter protected the sample from the intense infra-red radiation of the xenon flash light. The visible isotherm was photographed. An example of such a recording is seen in *Figure 3b.*

Representative parameters

T (chamber)	27° ± 1°C
T (sample)	27° ± 0.1°C
T (point source)	47° ± 0.1°C
Heating interval,	t 15–20 sec
Liquid crystal	'Thermomagic 28/30' (Merck),
T_1	28°C
T_2	30°C

Sample dimensions:

Length	2.0 cm
Width	1.0–1.8 cm
Thickness	0.08–0.15 cm

Narrow band-pass filter
Central wavelength 464 nm,
Half band width 17 nm

The thickness of the slabs should not exceed 1.5–2 x fold of the diameter of the contact area of the heat source. The reproducibility for measurements range from 2–5% in the isotropic and stretched samples, respectively.